Advances in Radiation Oncology (2020) **5**, 1286-1295

advances
in radiation oncology

www.advancesradonc.org

Scientific Article

MRI Radiomics for Prediction of Tumor Response and Downstaging in Rectal Cancer Patients after Preoperative Chemoradiation

Haihui Chen, MD,[a,b,1] Liting Shi, MS,[b,c,1] Ky Nam Bao Nguyen, MD,[b] Arta M. Monjazeb, MD,[b] Karen E. Matsukuma, MD,[d] Thomas W. Loehfelm, MD,[e] Haixin Huang, MD,[a] Jianfeng Qiu, PhD,[c,*] and Yi Rong, PhD[b,*]

[a]*Department of Medical Oncology, the Fourth Affiliated Hospital of Guangxi Medical University, Liuzhou, China;* [b]*Department of Radiation Oncology, University of California Davis School of Medicine, Sacramento, California;* [c]*Medical Engineering and Technology Research Center, Imaging-X Joint Laboratory, Department of Radiology, Shandong First Medical University & Shandong Academy of Medical Sciences, Taian, China;* [d]*Department of Pathology and Laboratory Medicine, University of California Davis School of Medicine, Sacramento, California; and* [e]*Department of Radiology, University of California Davis School of Medicine, Sacramento, California*

Received 21 January 2020; revised 7 April 2020; accepted 13 April 2020

Abstract

Purpose: This study aimed to investigate radiomic features extracted from magnetic resonance imaging (MRI) scans performed before and after neoadjuvant chemoradiotherapy (nCRT) in predicting response of locally advanced rectal cancer (LARC).

Methods and Materials: Thirty-nine patients who underwent nCRT for LARC were included, with 294 radiomic features extracted from MRI that was performed before (pre-CRT) and 6 to 8 weeks after completing nCRT (post-CRT). Based on tumor regression grade (TRG), 26 patients were classified as having a histopathologic good response (GR; TRG 0-1) and 13 as non-GR (TRG 2-3). Tumor downstaging (T-downstaging) occurred in 25 patients. Univariate analyses were performed to assess potential radiomic and delta-radiomic predictors for TRG in pathologic complete response (pCR) versus non-pCR, GR versus non-GR, and T-downstaging. The support vector machine-based multivariate model was used to select the best predictors for TRG and T-downstaging.

Results: We identified 13 predictive features for pCR versus non-pCR, 14 for GR versus non-GR, and 16 for T-downstaging. Pre-CRT gray-level run length matrix nonuniformity, pre-CRT neighborhood intensity difference matrix (NIDM) texture strength, and post-CRT NIDM busyness predicted all 3 treatment responses. The best predictor for GR versus non-GR was pre-CRT global minimum combined with clinical N stage in the multivariate analysis. The best predictor for T-downstaging was the combination of pre-CRT gray-level co-occurrence matrix correlation, NIDM-texture strength, and gray-level co-occurrence matrix variance. The pre-CRT, post-CRT, and delta radiomic-based models had no significant difference in predicting all 3 responses.

Conclusions: Pre-CRT MRI, post-CRT MRI, and delta radiomic-based models have the potential to predict tumor response after nCRT in LARC. These data, if validated in larger cohorts, can provide important predictive information to aid in clinical decision making.

Sources of support: This work had no specific funding.

Disclosures: Jianfeng Qiu and Liting Shi received grants from the Shandong Province Key Research and Development Program (2017GSF218075) and the Taishan Scholars Program of Shandong Province during the conduct of the study.

Research data are stored in an institutional repository and will be shared upon request to the corresponding author.

* Corresponding authors: Yi Rong, PhD and Jianfeng Qiu, PhD; E-mail: yrong@ucdavis.edu and jfqiu100@gmail.com

[1] Co-first authors.

https://doi.org/10.1016/j.adro.2020.04.016

Introduction

Colorectal cancer is the third most frequently diagnosed cancer and the fourth leading cause of cancer-related deaths worldwide.[1,2] Rectal cancer comprise about 27% to 58% of all colorectal cancers.[3] Neoadjuvant chemoradiotherapy (nCRT), followed by curative surgery, is the standard treatment for locally advanced rectal cancer (LARC). Recent outcome reports from 2 recent pooled analyses in a large cohort of patients with LARC showed that 15.6% to 24.4% of patients who underwent nCRT and surgical resection achieved a pathologic complete response (pCR),[4,5] raising the question of the necessity for subsequent radical surgery for this subset of patients. The watch-and-wait approach for patients with a clinical complete response after receiving nCRT or a local excision of the remaining scar tissue has demonstrated comparable oncologic outcomes to more invasive curative surgery, such as total mesorectal excision (TME).[6-8] Conversely, patients with more resistant disease may require more aggressive local therapy. There are limited data to aid in stratifying patients when making these treatment decisions.

An accurate assessment of treatment response to nCRT is important for a more conservative approach considering the high variation of response to nCRT.[9,10] Histopathology remains the gold standard to assess treatment response to nCRT, but with inherent limitations (eg, risk of surgical complications). For patients with a contraindication for surgery, research has focused on identifying noninvasive markers that can predict histologic regression. Magnetic resonance imaging (MRI) is the imaging modality of choice for the initial staging of rectal cancer[11]; however, routine MRI is known to perform poorly when assessing the pathologic response to nCRT owing to the inability to distinguish tumor desmoplasia and fibrosis from a viable tumor.[12,13]

Studies based on specialized MRI sequences, such as diffusion weighted imaging and dynamic contrast-enhanced MRI, have confirmed their high sensitivity and specificity in predicting a response to nCRT.[13-16] Yet, contradictory results have also been reported by other studies.[17,18] Specifically, Jang et al. reported that diffusion restriction remained in 42% of patients with pCR after nCRT and surgery.[19] Other challenges with MRI include an inability to assess important oncogenic features, such as angiogenesis or hypoxia, and the limited underlying tissue property information. Thus, extracting more information from MRI to predict an early assessment of a response to nCRT is desirable.

Radiomics is a quantitative texture analysis approach of diagnostic images for this purpose and focuses on extracting quantitative imaging features from specific annotated regions of interest (ROI) of medical images.[20,21] These features capture different characteristics of the ROIs, and describe tumor intensity, shape, size or volume, and other textures.[22,23] Human oncologic tissues exhibit strong signal differences that are assessable with imaging. The fundamental hypothesis is that radiomics can accurately quantify these differences with high dimensional imaging features, which may lead to imaging biomarkers with diagnostic, prognostic, or predictive powers.[21,24]

Published studies have shown promising results of the radiomics approach in predicting a pathologic response in non-small cell lung cancer using computed tomography (CT) images.[25,26] To the best of our knowledge, research with MRI radiomics for treatment response prediction in rectal cancer is limited, and early studies exclusively examined pre-CRT MRI.[27-29] Pre-CRT MRI radiomic studies aim to identify a subgroup of patients with LARC who may have a chance for a complete response but require intensification of the preoperative treatment.[28] Post-CRT MRI radiomics provides values to determine organ sensitivity to treatment, and thus assist with organ-preservation decision making before treatment.[30] Changes in radiomic features between pre- and post-CRT (ie, delta radiomics) may also be predictors of treatment response.[31] The best predictive timepoint for treatment response and clinical outcomes remains unknown.

In this present work, we investigated radiomic features extracted from MRI scans at different timepoints to predict LARC response to nCRT. Considering that tumor regression grade (TRG) and tumor-downstaging (T-downstaging) have become universally accepted metrics to assess tumor response to nCRT in LARC,[32] radiomic features extracted from MRI before and after nCRT and delta radiomics were assessed for their performance in predicting TRG and T-downstaging in patients with LARC who received nCRT followed by TME.

Methods and materials

Patient selection

Using an institutional review board–approved protocol, we retrospectively reviewed data on patients with LARC without distant metastases who were treated with nCRT between September 2010 and February 2018. A

total of 39 patients met the inclusion criteria (Supplementary Materials, Appendix E1) identified for this study.[33] Table 1 shows patients' clinical characteristics.

Pathology and tumor regression grade

A histopathologic assessment of the resection specimens was performed using a standardized protocol that included submission of the entire tumor bed if no mass-forming lesion was identified on gross examination.[34,35] Slides were reviewed by an experienced pathologist and further reviewed independently by a dedicated gastrointestinal pathologist, both blinded to the MRI data. Standard pathologic tumor staging of the resected specimen was performed in accordance with the guidelines of the American Joint Committee on Cancer (AJCC), 7th edition, 2010.[32]

pCR was defined as ypT0N0, extracted from the pathology reports of the surgical specimens. T-downstaging was defined as the lowering of the tumor classification from pre-CRT clinical stage (cT stage) to postoperative histopathologic stage (ypT stage), as defined by Prajnan et al.[36] In addition, the response of the primary tumor to radiation therapy was graded by the pathologist. The published 4-tier system adopted by the AJCC was used to avoid small categories in which TRG was determined by the amount of viable tumor, ranging from no evidence of any treatment effect (TRG 3), to a complete response with no viable tumor identified (TRG 0).[37]

For the analysis presented herein, patients were stratified to 2 therapeutic response groups: pCR versus nonpCR. Given the small number of cases in each TRG category, the AJCC TRG system was also used to stratify the patients into good responders (GR; defined as TRG 0-1) and nongood responders (non-GR; defined as TRG 2-3). The proportion of T-downstaging and TRG in 39 selected patients is shown in Table 1.

Table 1 Patient, tumor, and treatment characteristics

Characteristic	No. of patients (%)
Median age (range), y	60 (32-78)
Sex	
Men	22 (56.4)
Women	17 (43.6)
Clinical tumor classification	
cT2	4 (10.3)
cT3	24 (61.6)
cT4	10 (25.6)
Unknown	1 (2.6)
Clinical lymph node classification	
cN0	7 (17.9)
cN1-N2	32 (82.1)
Concurrent chemotherapy	
Protracted infusional 5-fluorouracil	32 (82.1)
Capecitabine uracil/tegafur	7 (17.9)
Pathology	
Adenocarcinoma	36 (92.3)
Mucinous adenocarcinoma	3 (7.7)
Histologic grade	
Well differentiated	11 (28.2)
Moderately differentiated	21 (53.8)
Unknown	7 (17.9)
Tumor-downstaging	
Yes	25 (64.1)
No	14 (35.9)
Tumor regression grade	
0	10 (25.6)
1	16 (41.0)
2	10 (25.6)
3	3 (7.7)

Image data sets, region of interest definition, and radiomic feature extraction

All patients underwent MRI scans for the rectum and pelvic cavity regions using a 1.5 T magnetic resonance scanner (Signa HDxt, GE Medical Systems) equipped with a phased-array coil. MRI scans were performed using a standardized MRI protocol in an oblique axial orientation, perpendicular to the long axis of the rectum at the site of the tumor. The pre- and post-CRT high-resolution T2-weighted images were analyzed in this study. The imaging parameters are listed in the Supplementary Materials, Appendix E2.[38,39] To reduce any bias relating to the time elapsed between completing nCRT and surgery, MRI for restaging and treatment response assessment was scheduled between the 6th and 8th week after completing nCRT.

Figure 1 illustrates the workflow of data acquisition and analysis in this study. The first step is ROI definition and segmentation. The ROI was defined as the whole tumor and rectum, excluding the intestinal lumen owing to the difficulty in definitively identifying viable tumor regions on routine MRI. In our study, pre- and post-CRT ROIs were segmented on the axial T2WI maps with the open-source software tool IBEX by a radiation oncologist with specific expertise in rectal cancer and who was blinded to the clinical and pathologic data.[1]

The second step is radiomic feature extraction from segmented ROIs using the IBEX software. A total of 294 radiomic features were extracted, including shape, first-order, high-order texture, and Laplacian of Gaussian filter-based features (Fig 1). The descriptions of the radiomic features are included in the supplementary materials (Appendix E3 and Table E1).

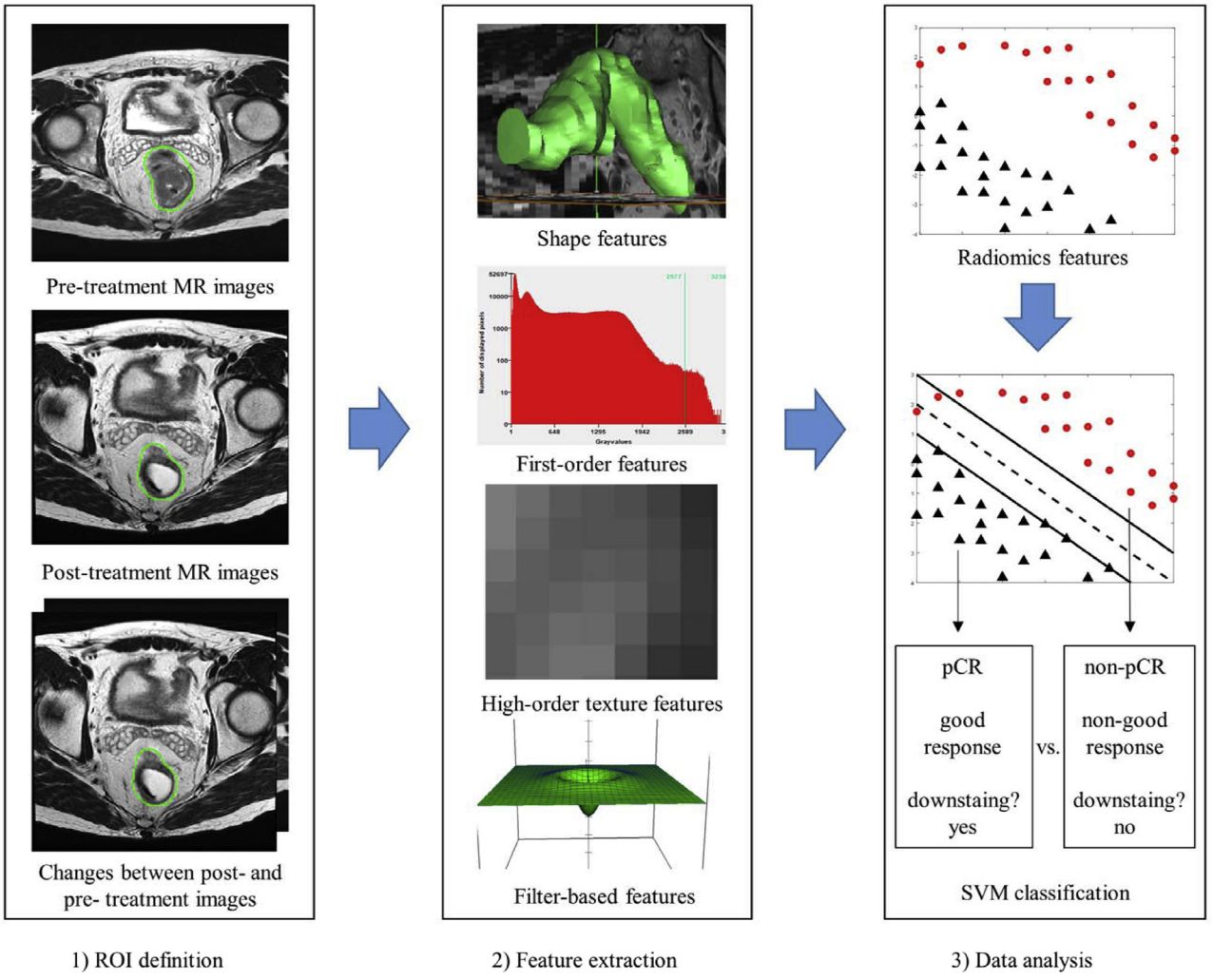

Figure 1 Data acquisition and analysis workflow. Region of interest definition: Regions of interest were defined by a radiation oncologist with specific expertise in rectal cancer. Feature extraction: Four categories of radiomic features were extracted: Shape, first-order, high-order texture, and filter-based features. Data analysis: The extracted radiomic features were used to predict clinical treatment response and tumor-downstaging using support vector machine classification.

The third step is to analyze the extracted features using the following steps.

Data normalization

To optimize the support vector machine (SVM) performance,[40] all data were normalized to the range in [0,1] using minimum (min)-maximum (max) normalization per the following equation:

$$f_i' = \frac{f_i - \min(f)}{\max(f) - \min(f)}$$

where $f = (f_1,\ldots,f_n)$ and is the i^{th} normalized data.

Dimension reduction and univariate analysis

After normalization, independent features were identified to reduce data dimension. A Wilcoxon rank sum test was used to quantify the differences in all features between the 2 groups of patients (TRG prediction: pCR vs non-pCR, GR vs non-GR; downstaging prediction: yes vs no). Spearman's correlation coefficient (r_s) was calculated between different pairs of features. Within any pair with $r_s > 0.8$, the feature with the lower P-value in the Wilcoxon rank sum test was selected for the subsequent analysis. Among the selected features, a P-value $< .05$ was considered statistically significant.

SVM-based multivariate classification

A SVM-based multivariate model was used to select the best predictors for TRG and T-downstaging (Fig E1). The SVM model was fitted using Gaussian kernel with the kernel scale automatically selected by the heuristic procedure. The evaluated potential radiomic predictors included features extracted from pre- and post-CRT images and the relative changes in these features (ie, delta-radiomic features). The following potential clinical

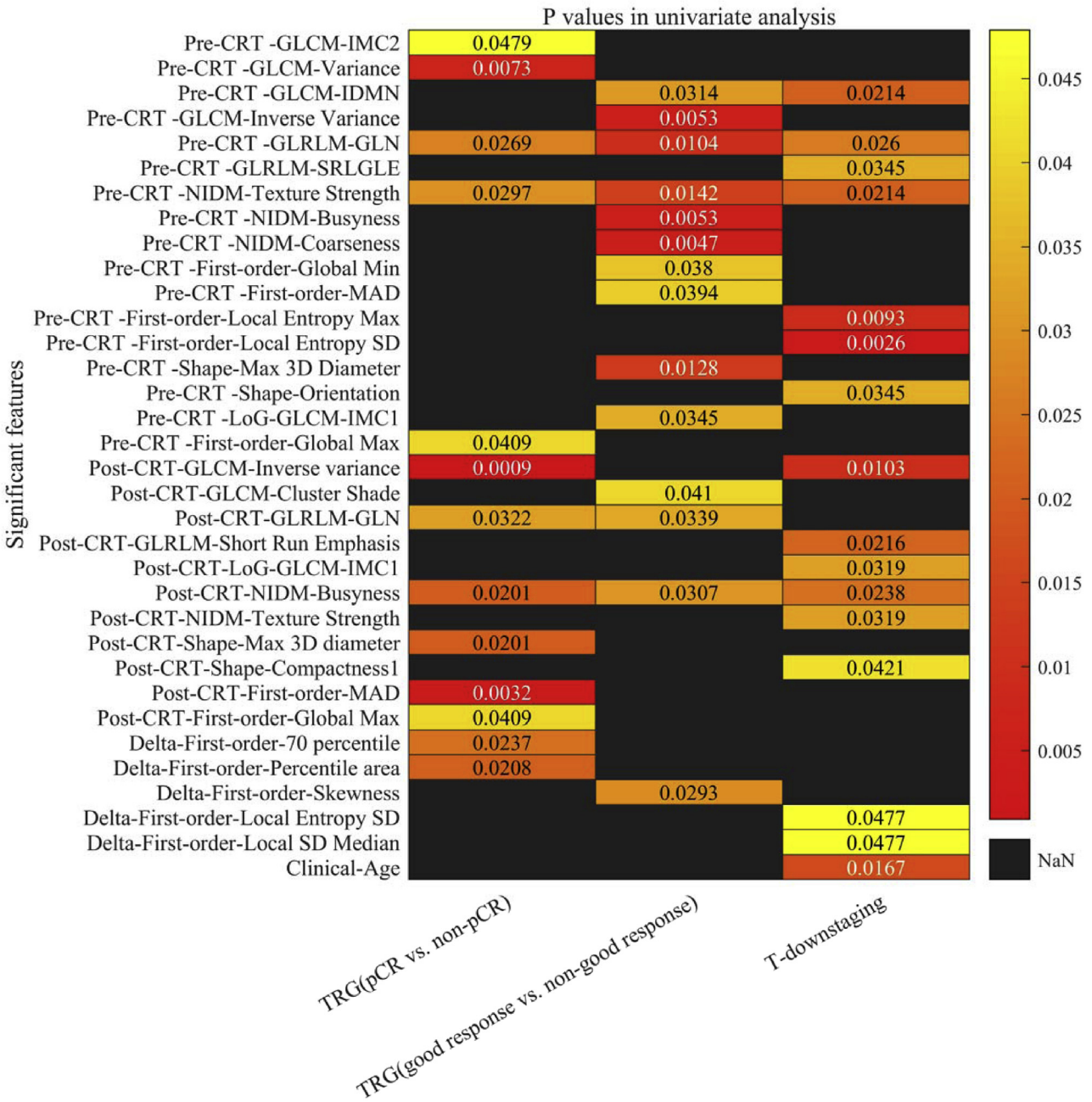

Figure 2 The significant features ($P < .05$) heat map generated using their P values in the univariate analysis. NA represents that the feature on the y axis is not significant to predict a response on the x axis ($P \geq .05$). *Abbreviations:* GLCM = gray-level co-occurrence matrix; GLN = gray-level nonuniformity; GLRLM = gray-level run length matrix; HoG = histogram of gradient orientations; IDMN = inverse difference moment normalized; IMC = informational measure of correlation; MAD = median absolute deviation; NIDM = neighborhood intensity difference matrix; SD = standard deviation; SRLGLE = shortrun low-gray level emphasis.

predictors were also evaluated: Age, sex, clinical T classification, clinical lymph node (N) classification, grade, and type of chemotherapy.

Among the 39 eligible patients, 26 with both pre- and post-CRT images were added in the training set; 7 with only pre-CRT images and 6 with only post-CRT images were added in the test set of pre- and post-CRT radiomic models, respectively. The selection of best predictors was performed using the training data. Leave-one-out validation was used to evaluate the classification performance in this process. The performance between any 2 of pre-CRT, post-CRT, and delta radiomic-based multivariate models in the training data set was compared using a permutation test with 5000 permutations, where a P-value $< .05$ was considered statistically significant. All analyses were performed with MATLAB 2015b.

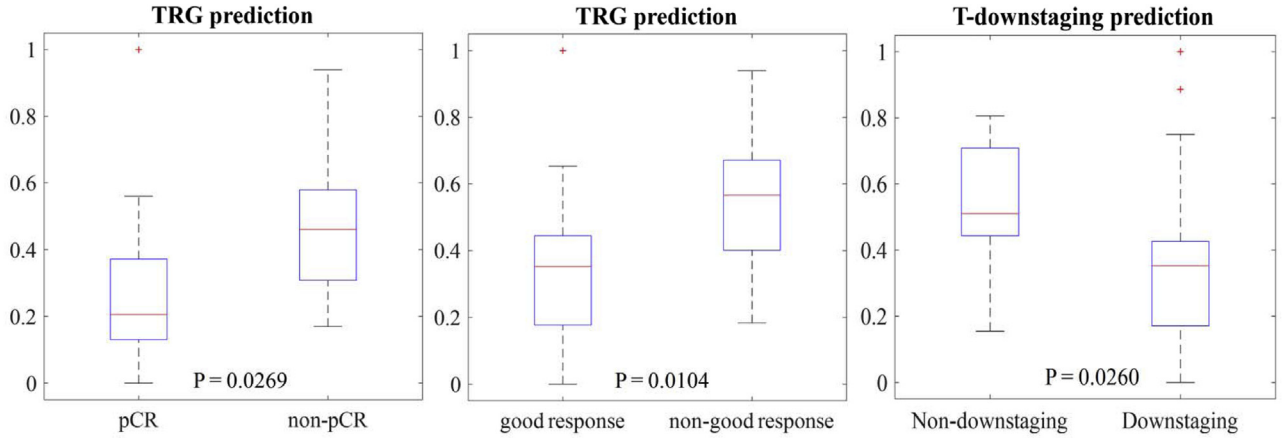

Figure 3 Box plots for pre-chemoradiotherapy gray-level run length matrix-gray-level nonuniformity for the 2 groups of patients in tumor regression grade and tumor-downstaging prediction. Each box represents the interquartile range. The line inside the box represents the median. The upper and lower whiskers extend to the highest and lowest values within 1.5 × interquartile range of the 0.75 and 0.25 quartiles, respectively. The plus sign represents outlier.

Results

Dimension reduction

Of the 294 radiomic features, 38 independent features were selected for the subsequent analysis. Features were selected based on the differences between the 2 groups of patients with respect to the treatment response. Thus, the selected features were distinctive for different treatment response prediction.

Univariate analysis

In the univariate analysis, radiomic features extracted from pre- and post-CRT images and their changes were significantly correlated with TRG and T-downstaging (Fig 2). A total of 13, 14, and 16 features were predictive of TRG pCR versus non-pCR, TRG GR versus non-GR, and T-downstaging, respectively (P = .0009-.0479, .0047-.041, and .0026-.0477, respectively). The best predictors for each treatment response were post-CRT gray level co-occurrence matrix (GLCM)-inverse variance for pCR versus non-Pcr; pre-CRT NIDM-coarseness for GR versus non-GR; and pre-CRT first-order local entropy standard deviation (SD) for T-downstaging, respectively (P = .0009, .0047, and .0026, respectively).

Overall, pre-CRT gray-level run length matrix (GLRLM)–gray level nonuniformity (GLN), pre-CRT NIDM-texture strength, and post-CRT NIDM-busyness can predict all 3 treatment responses at $P < .05$. Figure 3 shows the box plots for pre-CRT GLRLM-GLN in the 2 groups of patients for TRG and T-downstaging prediction.

None of the clinical factors was significantly correlated with TRG pCR versus non-pCR and T-downstaging. Only 1 clinical factor (age) significantly correlated with TRG GR versus non-GR (P = .0167).

SVM-based multivariate classification

The best predictors for pCR versus non-pCR were the combination of features in different categories (Table 2). The pre-CRT GLRLM-GLN was able to classify pCR group and non-pCR groups independently with the training data accuracy at 88.5%, classification loss = 0.1154, and test data accuracy at 57.1%. When combined with the pre-CRT maximum 3-dimensional diameter, the classification performance was highly improved (training data: Accuracy = 92.3%, classification loss = .0769; test data: 57.1%). The best predictors for GR versus non-GR were pre-CRT global minimum combined with clinical N stage in the multivariate analysis (training data: accuracy = 100%, classification loss = .0769; test data: accuracy = 100%; Table 2).

The best predictor for T-downstaging is the combination of pre-CRT GLCM-correlation, NIDM-texture strength, and GLCM-variance (training data: Accuracy = 92.3%, classification loss = .1154; test data: Accuracy = 71.4%). In addition, post-CRT NIDM-busyness was an independent predictor for T-downstaging and performed best in the post-CRT radiomic features (training data: accuracy = 92.3%, classification loss = .2308; test data: accuracy = 50.0%; Table 2).

The pre-CRT, post-CRT, and delta radiomic-based models had no significant difference ($P > .29$) in predicting pCR versus non-pCR, GR versus non-GR, and T-downstaging in the permutation test (Table E2).

Table 2 Best predictors for TRG and tumor-downstaging prediction and their performance in support vector machine-based multivariate classification

Response	Images	Best predictors	Training data		Test data
			Accuracy	Class loss	Accuracy
TRG (pCR vs non-pCR)	Pre-CRT	GLRLM-GLN and shape-maximum 3-dimensional diameter	92.3%	0.0769	57.1%
	Post-CRT	Clinical tumor stage and HoG-percentile area	88.46%	0.1538	66.7%
	Delta	GLCM-cluster shade and HoG-percentile and maximum probability	96.15%	0.0769	—
TRG (GR vs non-GR)	Pre-CRT	Global minimum and clinical node stage	100%	0.0769	100%
	Post-CRT	Clinical node stage and 0.025 quantile and local entropy minimum	100%	0.1154	83.3%
	Delta	Clinical node stage and GLRLM-LRLGLE	92.3%	0.0769	—
Tumor-downstaging (yes vs no)	Pre-CRT	GLCM-correlation and NIDM-texture strength and GLCM variance	92.3%	0.1154	71.4%
	Post-CRT	NIDM busyness	92.3%	0.2308	50.0%
	Delta	Shape orientation	92.3%	0.1154	—

Abbreviations: CRT = chemoradiotherapy; GLCM = gray-level co-occurrence matrix; GLRLM = gray-level run length matrix; GR = good response; HoG = histogram of gradient orientations; LRLGLE = long-run low gray-level emphasis; NIDM = neighborhood intensity difference matrix; pCR = pathologic complete response; TRG = tumor regression grade.

Discussion

In the present study, the pCR rate of primary LARC treated curatively with nCRT was 23.1%, which was consistent with results reported by the MD Anderson Cancer Center (27%) and Creighton University (22%).[41,42] An additional 24 patients (61.5%) showed evidence of T-downstaging of tumor after nCRT. Alternative and less invasive treatment options for sphincter or organ preservation could potentially be considered for these patients. Our study has 13 patients (33.3%) with non-GR (TRG 2-3), of which 1 patient (7.7%) showed poor response (TRG 3). Early detection of poor nCRT responders would facilitate physician decision making. Being able to define which patients are likely to be poor responders would allow for alternative methods to be tested, such as targeted therapy, immunotherapy, or more aggressive preoperative regimens (eg, dose escalation, total neoadjuvant therapy, or alternative chemotherapy agents). Hence, the ability to correctly predict responses to preoperative therapy can be beneficial for patient-tailored treatment strategies.[43,44]

Radiomic features extracted from MRI have been demonstrated to be highly significant predictors of nCRT in LARC.[27-29] However, most of the work focused on single-category radiomic features from MRI, which may have inherent limitations in their predictive power. Nie et al[27] assessed GLCM features in predicting a response to neoadjuvant therapy with 48 patient data sets, and found that voxelized heterogeneity models outperformed conventional volume-based metrics in predicting pCR with improved area under the receiver operating characteristic curve.

Similar results were found for the GR prediction. Dinapoli et al[28] found that the most significant features from pretreatment T2 MRI in LARC to predict pCR were skewness with $\sigma = 0.485$ mm (SKE0485) and entropy with $\sigma = 0.344$ mm (ENT0344), but no significant prediction power was observed with kurtosis. Cusumano et al[29] reported that the fractal parameters of the subpopulations had the highest performance in predicting pCR. The major findings of our present work include identifying 13, 14, and 16 significant predictive features, including shape, first-order, high-order texture, and Laplacian of Gaussian features for pCR versus non-pCR, GR versus non-GR, and T-downstaging, respectively. Most importantly, we found that the best predictors for TRG and T-downstaging were the combined features in different categories (ie, prediction accuracy for TRG [pCR vs non-pCR] improved from 88.5% to 92.3% after combining the pre-CRT maximum 3-dimensional diameter [conventional feature] with pre-CRT GLRLM-GLN [texture feature]). Our results agree with the findings and models presented by previous publications.[27]

Another major contribution from the present study is the evaluation of radiomic features extracted from pre-CRT MRI, post-CRT MRI, and the feature changes between these two (delta-radiomics). So far in the literature, radiomic studies on LARC mostly focused on either pre- or post-CRT MRI separately. Three recent studies with

small-size samples have demonstrated the pCR prediction power in patients with LARC using pre-CRT MRI radiomic features alone.[27-29] MRI radiomic features in predicting a pathologic response after nCRT for LARC were also verified in 3 separate studies, using post-CRT MRI,[45] both pre-CRT, and post-CRT MRI,[30] or delta-radiomic MRI features.[31]

The significance of combining all 3 in 1 study is that radiomic features at different time points may increase the specificity for response prediction. To the best of our knowledge, this is the first study using pre-CRT MRI, post-CRT MRI, and delta-radiomic features analyses to predict TRG and T-downstaging for LARC. Our results revealed that the pre-CRT, post-CRT, and delta radiomic-based models had no significant difference in TRG prediction for pCR versus non-pCR, GR versus non-GR, and T-downstaging in the permutation test. This means that the pre-CRT MRI-based radiomic model is sufficient for patient-tailored nCRT strategies for the best treatment response prediction.

Post-CRT MRI directly reflects the status of the tumor after nCRT, which is more relevant to the surgical pathology and helpful for the purpose of organ-preservation decision. When significant clinical downstaging occurs after nCRT for patients with LARC, some patients may be considered for local excision rather than curative TME to preserve the anal sphincter and reduce morbidity.[46] Thus, the radiomic feature performance for T-downstaging is also of clinical concern for operative method selection. In this study, we found that 4 post-CRT radiomic features and 2 delta radiomic features can predict T-downstaging, but not for pCR versus non-pCR or GR versus non-GR. Overall, among the 33 selected features, 11 features from post-CRT MRI are of great value in accurately identifying patients for whom a less invasive surgery may be the most appropriate.

The limitations of this analysis should be noted. First, this study was retrospective in nature with a relatively small sample size. The published 4-tier AJCC TRG system was used to avoid small categories.[37] Given the small number of cases in each TRG category, the AJCC TRG system was also used to stratify patients into groups of GR and non-GR. Further research with a larger patient cohort is needed to confirm these results. Second, all patients were from a single center without external validation. To minimize bias, we performed an internal validation by setting patients with both pre- and post-CRT images as training data and patients with only pre- or post-CRT images as test data for pre- and post-CRT radiomic- based prediction. To ensure the prediction accuracy and consistency of the pre-CRT, post-CRT, and delta radiomic models, the selection of the best predictors was performed using the training data, but a leave-one-out validation was used to evaluate the classification performance in this process.

SVM-based multivariate classification was used instead of the conventional logistic regression analysis due to its capacity to model complex relationships between independent and predictor variables, allowing for the inclusion of a large number of variables. Nevertheless, further multicenter studies with external validation are needed to validate the reported data and provide a better generalization of our results. In addition, this study cohort only received nCRT without other neoadjuvant chemotherapy. Future studies should examine patients treated with neoadjuvant multiagent chemotherapy using a total neoadjuvant therapy approach.

Conclusions

To our knowledge, this is the first study to focus on the relationship between pathologic response after nCRT and radiomic features extracted from pre-CRT MRI, post-CRT MRI, and delta-radiomic features in LARC. Our findings confirm that radiomic features extracted from pre-CRT MRI, post-CRT MRI, and delta-radiomic features could potentially be helpful for TRG predication in pCR versus non-pCR, TRG GR versus non-GR, and T-downstaging after nCRT in LARC. We also showed that the pre-CRT, post-CRT, and delta radiomic-based models demonstrated the same ability in therapeutic response prediction, which means that MRI obtained pre- and post-CRT can be used for response prediction. Future well-designed prospective trials with larger patient and external validation cohorts are needed to verify our results.

Supplementary data

Supplementary material for this article can be found at https://doi.org/10.1016/j.adro.2020.04.016.

References

1. Sauer R, Becker H, Hohenberger W, et al. Preoperative versus postoperative chemoradiotherapy for rectal cancer. *N Engl J Med*. 2004;351:1731-1740.
2. Valentini V, Glimelius B, Haustermans K, et al. EURECCA consensus conference highlights about rectal cancer clinical management: The radiation oncologist's expert review. *Radiother Oncol*. 2014;110:195-198.
3. Brenner H, Bouvier AM, Foschi R, et al. Progress in colorectal cancer survival in Europe from the late 1980s to the early 21st century: The EUROCARE study. *Int J Cancer*. 2012;131:1649-1658.
4. Maas M, Nelemans PJ, Valentini V, et al. Long-term outcome in patients with a pathological complete response after chemoradiation for rectal cancer: A pooled analysis of individual patient data. *Lancet Oncol*. 2010;11:835-844.
5. Martin ST, Heneghan HM, Winter DC. Systematic review and meta-analysis of outcomes following pathological complete response to

neoadjuvant chemoradiotherapy for rectal cancer. *Br J Surg*. 2012; 99:918-928.
6. Maas M, Beets-Tan RG, Lambregts DM, et al. Wait-and-see policy for clinical complete responders after chemoradiation for rectal cancer. *J Clin Oncol*. 2011;29:4633-4640.
7. Shin YS, Yu CS, Park JH, et al. Total mesorectal excision versus local excision after favorable response to preoperative chemoradiotherapy in "early" clinical T3 rectal cancer: A propensity score analysis. *Int J Radiat Oncol Biol Phys*. 2017;99:136-144.
8. Smith RK, Fry RD, Mahmoud NN, Paulson EC. Surveillance after neoadjuvant therapy in advanced rectal cancer with complete clinical response can have comparable outcomes to total mesorectal excision. *Int J Colorectal Dis*. 2015;30:769-774.
9. Fokas E, Liersch T, Fietkau R, et al. Tumor regression grading after preoperative chemoradiotherapy for locally advanced rectal carcinoma revisited: Updated results of the CAO/ARO/AIO-94 trial. *J Clin Oncol*. 2014;32:1554-1562.
10. Benzoni E, Intersimone D, Terrosu G, et al. Prognostic value of tumor regression grading and depth of neoplastic infiltration within the perirectal fat after combined neoadjuvant chemo-radiotherapy and surgery for rectal cancer. *J Clin Pathol*. 2006;59:505-512.
11. Beets-Tan RG, Lambregts DM, Maas M, et al. Magnetic resonance imaging for the clinical management of rectal cancer patients: Recommendations from the 2012 European Society of Gastrointestinal and Abdominal Radiology (ESGAR) consensus meeting. *Eur Radiol*. 2013;23:2522-2531.
12. Lee JH, Jang HS, Kim JG, et al. Prediction of pathologic staging with magnetic resonance imaging after preoperative chemoradiotherapy in rectal cancer: Pooled analysis of KROG 10-01 and 11-02. *Radiother Oncol*. 2014;113:18-23.
13. van der Paardt MP, Zagers MB, Beets-Tan RG, Stoker J, Bipat S. Patients who undergo preoperative chemoradiotherapy for locally advanced rectal cancer restaged by using diagnostic MR imaging: A systematic review and meta-analysis. *Radiology*. 2013;269:101-112.
14. Lambrecht M, Vandecaveye V, De Keyzer F, et al. Value of diffusion-weighted magnetic resonance imaging for prediction and early assessment of response to neoadjuvant radiochemotherapy in rectal cancer: Preliminary results. *Int J Radiat Oncol Biol Phys*. 2012;82:863-870.
15. Oberholzer K, Menig M, Pohlmann A, et al. Rectal cancer: Assessment of response to neoadjuvant chemoradiation by dynamic contrast enhanced MRI. *J Magn Reson Imaging*. 2013;38: 119-126.
16. Intven M, Reerink O, Philippens ME. Dynamic contrast enhanced MR imaging for rectal cancer response assessment after neoadjuvant chemoradiation. *J Magn Reson Imaging*. 2015;41:1646-1653.
17. Joye I, Deroose CM, Vandecaveye V, Haustermans K. The role of diffusion-weighted MRI and (18)F-FDG PET/CT in the prediction of pathologic complete response after radiochemotherapy for rectal cancer: a systematic review. *Radiother Oncol*. 2014;113:158-165.
18. Maas M, Lambregts DM, Nelemans PJ, et al. Assessment of clinical complete response after chemoradiation for rectal cancer with digital rectal examination, endoscopy, and MRI: Selection for organ-saving treatment. *Ann Surg Oncol*. 2015;22:3873-3880.
19. Jang KM, Kim SH, Choi D, Lee SJ, Park MJ, Min K. Pathological correlation with diffusion restriction on diffusion-weighted imaging in patients with pathological complete response after neoadjuvant chemoradiation therapy for locally advanced rectal cancer: Preliminary results. *Br J Radiol*. 2012;85:e566-e572.
20. Lambin P, Rios-Velazquez E, Leijenaar R, et al. Radiomics: Extracting more information from medical images using advanced feature analysis. *Eur J Cancer*. 2012;48:441-446.
21. Kumar V, Gu Y, Basu S, et al. Radiomics: The process and the challenges. *Magn Reson Imaging*. 2012;30:1234-1248.
22. Gillies RJ, Kinahan PE, Hricak H. Radiomics: Images are more than pictures, they are data. *Radiology*. 2016;278:563-577.
23. Parekh V, Jacobs MA. Radiomics: A new application from established techniques. *Expert Rev Precis Med Drug Dev*. 2016;1: 207-226.
24. Panth KM, Leijenaar RT, Carvalho S, et al. Is there a causal relationship between genetic changes and radiomics-based image features? An in vivo preclinical experiment with doxycycline inducible GADD34 tumor cells. *Radiother Oncol*. 2015;116: 462-466.
25. Coroller TP, Agrawal V, Narayan V, et al. Radiomic phenotype features predict pathological response in non-small cell lung cancer. *Radiother Oncol*. 2016;119:480-486.
26. Huynh E, Coroller TP, Narayan V, et al. CT-based radiomic analysis of stereotactic body radiation therapy patients with lung cancer. *Radiother Oncol*. 2016;120:258-266.
27. Nie K, Shi L, Chen Q, et al. Rectal cancer: Assessment of neoadjuvant chemoradiation outcome based on radiomics of multiparametric MRI. *Clin Cancer Res*. 2016;22:5256-5264.
28. Dinapoli N, Barbaro B2, Gatta R, et al. Magnetic resonance, vendor-independent, intensity histogram analysis predicting pathologic complete response after radiochemotherapy of rectal cancer. *Int J Radiat Oncol Biol Phys*. 2018;102:765-774.
29. Cusumano D, Dinapoli N, Boldrini L, et al. Fractal-based radiomic approach to predict complete pathological response after chemoradiotherapy in rectal cancer. *Radiol Med*. 2018;123:286-295.
30. Liu Z, Zhang XY, Shi YJ, et al. Radiomics analysis for evaluation of pathological complete response to neoadjuvant chemoradiotherapy in locally advanced rectal cancer. *Clin Cancer Res*. 2017;23: 7253-7262.
31. Boldrini L, Cusumano D, Chiloiro G, et al. Delta radiomics for rectal cancer response prediction with hybrid 0.35 T magnetic resonance-guided radiotherapy (MRgRT): A hypothesis-generating study for an innovative personalized medicine approach. *Radiol Med*. 2019;124:145-153.
32. Edge SB, Compton CC. The American Joint Committee on Cancer: The 7th edition of the AJCC cancer staging manual and the future of TNM. *Ann Surg Oncol*. 2010;17:1471-1474.
33. Bosman FT, Carneiro F, Hurban RH, Theise ND, eds. *WHO classification of tumours of the digestive system*. 4th ed. Geneva, Switzerland: World Health Organization; 2010.
34. Lester SC. *Manual of surgical pathology*. 2nd ed. Philadelphia, PA: Elsevier Churchill Livingstone; 2006:334-344.
35. Westra WH, Hruban RH, Phelps TH, Isacson C. *Surgical pathology dissection*. 2nd ed. New York, NY: Springer Science; 2003:70-73.
36. Das P, Skibber JM, Rodriguez-Bigas MA, et al. Predictors of tumor response and downstaging in patients who receive preoperative chemoradiation for rectal cancer. *Cancer*. 2007;109:1750-1755.
37. Trakarnsanga A, Gonen M, Shia J, et al. Comparison of tumor regression grade systems for locally advanced rectal cancer after multimodality treatment. *J Natl Cancer Inst*. 2014;106.
38. Zhang L, Fried DV, Fave XJ, Hunter LA, Yang J, Court LE. IBEX: An open infrastructure software platform to facilitate collaborative work in radiomics. *Med Phys*. 2015;42:1341-1353.
39. Pallavi T, Prateek P, Lisa R, Leo W, Chaitra B, Andrew S, et al. Texture descriptors to distinguish radiation necrosis from recurrent brain tumors on multi-parametric MRI. *Proc SPIE Int Soc Opt Eng*. 2014;9035:90352B.
40. Juszczak P, Tax DMJ, Duin RPW. Feature scaling in support vector data description. *Machine Learning*. 2007;54:45-66.
41. Janjan NA, Khoo VS, Abbruzzese J, et al. Tumor downstaging and sphincter preservation with preoperative chemoradiation in locally advanced rectal cancer: The MD Anderson Cancer Center experience. *Int J Radiat Oncol Biol Phys*. 1999;44:1027-1038.
42. Adams DR, Blatchford GJ, Lin KM, Ternent CA, Thorson AG, Christensen MA. Use of preoperative ultrasound staging for treatment of rectal cancer. *Dis Colon Rectum*. 1999;42:159-166.

43. Bökkerink GMJ, de Graaf EJR, Punt CJA, et al. The CARTS study: Chemoradiation therapy for rectal cancer in the distal rectum followed by organ-sparing transanal endoscopic microsurgery. *BMC Surg*. 2011;11:34.
44. Beets GL, Figueiredo NL, Habr-Gama A, van de Velde CJ. A new paradigm for rectal cancer: Organ preservation: Introducing the International Watch & Wait Database (IWWD). *Eur J Surg Oncol*. 2015;41:1562-1564.
45. Horvat N, Veeraraghavan H, Khan M, et al. MR imaging of rectal cancer: Radiomics analysis to assess treatment response after neoadjuvant therapy. *Radiology*. 2018;287:833-843.
46. Rullier E, Vendrely V, Asselineau J, et al. Organ preservation with chemoradiotherapy plus local excision for rectal cancer: 5-year results of the GRECCAR 2 randomised trial. *Lancet Gastroenterol Hepatol*. 2020;5:465-474.